



Ratiometric multimodal chemosensors based on cubic silsesquioxanes for monitoring solvent polarity

Kazuo Tanaka, Kenichi Inafuku, Yoshiki Chujo *

Department of Polymer Chemistry, Graduate School of Engineering, Kyoto University, Katsura, Nishikyo-ku, Kyoto 615-8510, Japan

ARTICLE INFO

Article history:

Received 28 August 2008

Revised 4 October 2008

Accepted 7 October 2008

Available online 11 October 2008

Keywords:

Multimodal probe

Silsesquioxane

^{19}F NMR

Fluorescence

Ratiometric sensor

Solvent polarity

ABSTRACT

We report the multi-functionalized cubic silsesquioxane (POSS) as the ratiometric multimodal chemosensors for monitoring solvent polarity with fluorescence and ^{19}F NMR. The alteration of the dispersion state of the modified POSS by changing solvent polarity can be reflected into the orthogonal signal responses for the fluorescence and ^{19}F NMR. In addition, the ratiometric dual monitoring for the enzymatic reaction was performed using the POSS-based chemosensor.

© 2008 Elsevier Ltd. All rights reserved.

1. Introduction

Magnetic resonance imaging (MRI) is one of powerful diagnostic tools for modern clinical medicine, and ^{19}F MRI using the fluorinated compounds as contrast agents has recently gathered attentions not only for acquiring spatial information but also for monitoring vital reactions.¹ A combination of several simultaneous detection techniques can ensure a better reliability and a rapid diagnosis due to the elimination of the troublesome task to correct distortions or lags in the images caused by respirations or strokes.² Especially, the ^{19}F MRI/fluorescence multimodal imaging system has benefits, for example, for in vivo small-animal imaging which is a prerequisite step before clinical application as well as for a very useful tool for biomedical investigation.³ Thus, the multimodal imaging agents have been strongly desired for extracting chemical information from in vivo with higher accuracy and specificity.

Ratiometric fluorescence probes which exhibit signal enhancement at one emission band and reduction at another band by the target recognition can decrease the disordering factors such as photobleaching, fluctuation of the source intensity, sensitivity of the instrument, and artifacts associated with the probe concentration and environment.⁴ Many efforts have been made to synthesize ratiometric fluorescent sensors for biological events or environmental factors, however, to our knowledge, the ratiometric chemosensors in different detection modalities have been less reported.⁵

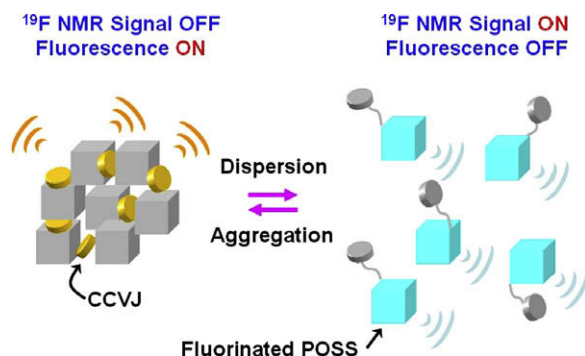
Cubic octameric polyhedral oligomeric silsesquioxanes (POSS) are water-soluble rigid nanoblocks, and POSS-based compounds showed superior biocompatibility such as less toxicity and good stability.⁶ Therefore, POSS are promised to be a good scaffold to assemble functional molecules for the multimodal detection.⁷ Herein, we synthesized the multi-functionalized cubic silsesquioxane (POSS) as the ratiometric multimodal chemosensors for monitoring solvent polarity. The alteration of the dispersion state of the modified POSS by changing solvent polarity can be reflected into the orthogonal signal responses for the fluorescence and ^{19}F NMR. In addition, the ratiometric multimodal monitoring for the enzymatic reaction was performed using the POSS-based chemosensor.

2. Results and discussion

Scheme 1 summarizes the principle for monitoring solvent polarity. Several considerations influence the design of the ratiometric multimodal chemosensor. The molecular rotor CCVJ (**2**)⁸ which can show strong emission under higher viscosity circumstances due to the suppression of non-radiative process via internal molecular rotation was incorporated into the modified POSS (C-POSS) as a fluorescent signal moiety. Under the higher polar conditions, though the cluster of C-POSS can be formed, they can maintain dispersion state without precipitation. Low tumbling and steric hindrance in the cluster could enhance the emission from the CCVJ moiety and reduce the sensitivity of ^{19}F NMR signals from the trifluoroacetyl groups^{1h} in the probe. In contrast, under

* Corresponding author. Tel.: +81 75 383 2604; fax: +81 75 383 2605.

E-mail address: chujo@chujo.synchem.kyoto-u.ac.jp (Y. Chujo).



Scheme 1. Detection mechanism of C-POSS for solvent polarity.

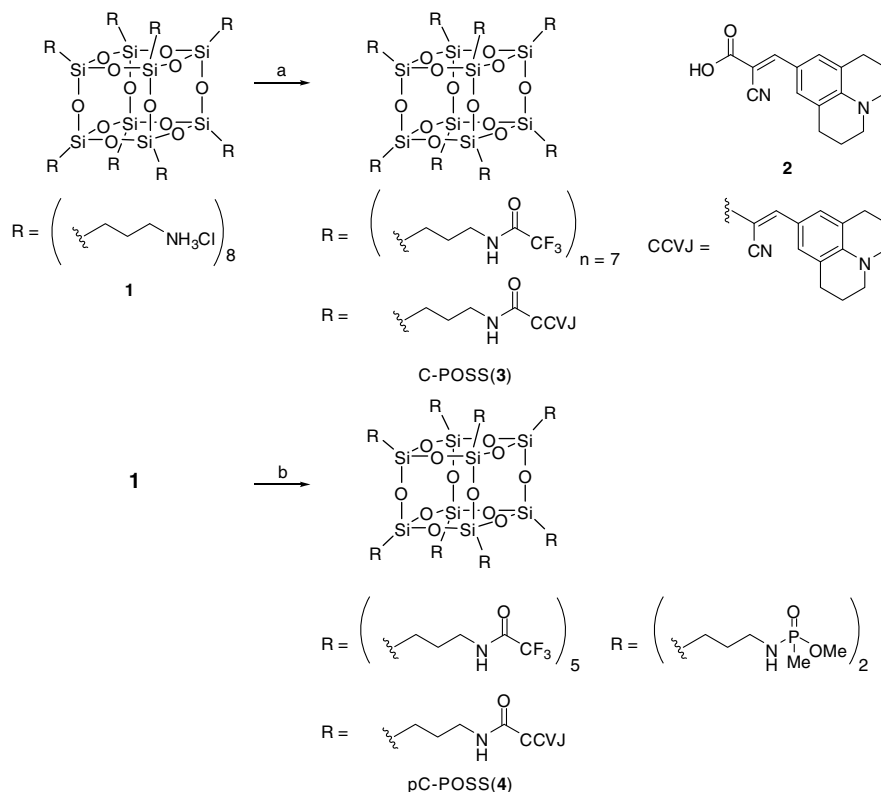
the lower polar conditions, the decrease of fluorescence and the enhancement of ^{19}F NMR signals would be induced by recovering the free rotation of C-POSS. These behaviors toward mobility are the key for acquiring the ratiometric response of C-POSS derivatives.

The synthesis of the modified POSS probes is outlined in Scheme 2. The modification of POSS with the signal moieties are accomplished using octaammonium POSS (**1**) as a starting material.⁹ The introduction of trifluoroacetyl groups and the fluorophore into POSS proceeded in good yield and subsequent dialysis in water was executed for the purification.¹⁰ We also prepared the phosphorylated C-POSS (pC-POSS) for monitoring the enzymatic reaction. The methanol–water solvent system can regulate polarity by the mixing ratio without significant changing of viscosity.^{11,12} Less influence on the emission intensity of the free CCVJ **2** by the addition of methanol in the aqueous solutions suggests that the effect of viscosity changing on the fluorescence property of

C-POSS could be ignored.¹³ Similar extent of the absorption of C-POSS at 350 nm with various concentrated methanol represents that undesired precipitation should be less generated by the addition of methanol under 250 μM concentration of C-POSS.¹⁴ These results indicate that the POSS should be crucially responsible for the formation of the cluster depending on solvent polarity. In addition, the degradation of C-POSS and pC-POSS was not observed after 24 h incubation at 37 $^{\circ}\text{C}$ at pH 7.0 in the presence of proteinase K. These results imply that the modified POSS could avoid undesired digestion under biological conditions.

The solutions containing 250 μM C-POSS with various concentrated methanol in 50 mM sodium phosphate buffer (pH 7.0) were prepared, and ^{19}F NMR signals of these solutions were monitored (Table 1). The strong signals were obtained from the 75 and 100 wt% methanol samples. The peak height was enhanced by the increase of methanol concentration. In contrast to the tendency of ^{19}F NMR signals, the emission band at 500 nm with the excitation at 350 nm, which corresponded to that of the free CCVJ **2**, was reduced by the increase of methanol concentration (Fig. 1). The lower level of fluorescence intensity was observed from the 75 and 100 wt% methanol solutions. Figure 2 demonstrates the fluorescence image and the one-dimensional ^{19}F NMR spectra. These results clearly indicate the ratiometric response toward polarity in ^{19}F NMR and fluorescence spectra. Although the sensitivity of the probe for acquiring clear contrasts in the ^{19}F MR image was lower than for the fluorescence image, our system could have a possibility to improve sensitivity by employing POSS-core dendrimers for incorporating the larger number of fluorine atoms into the probe.

In order to clarify the cluster formation of C-POSS in various methanol concentrations, dynamic light scattering (DLS) measurements were executed (Fig. 3). The solutions containing 75 wt% and 100 wt% methanol gave less significant scattering, and the r_{H} value was not determined. On the other hand, from the solution contain-

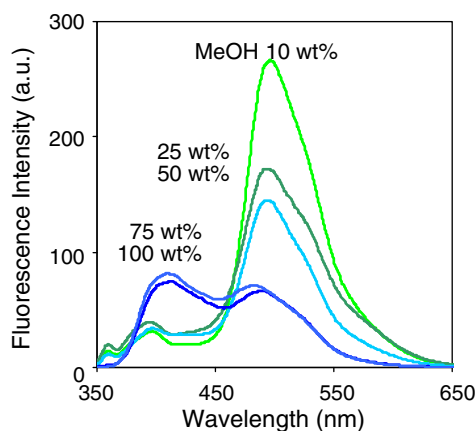
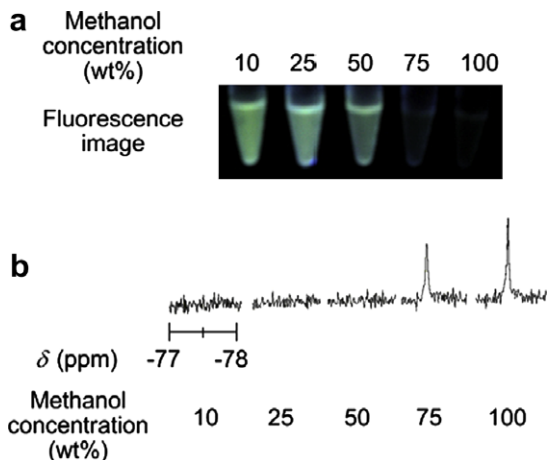


Scheme 2. Reagents: (a) i-ethyl trifluoroacetate (7 eq.), triethylamine, methanol; ii-**2**, DMT-MM, 21%; (b) i-ethyl trifluoroacetate (5 eq.), triethylamine, methanol; ii-**2**, DMT-MM; iii-methylphosphinic dichloride, triethylamine, chloroform, 30%.

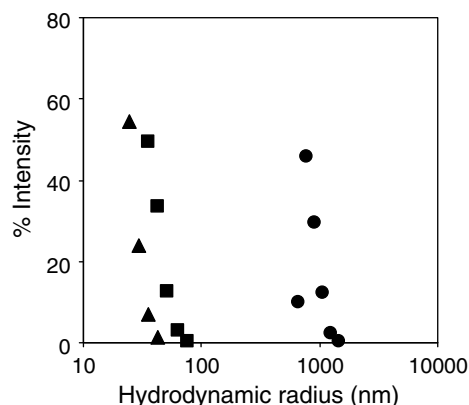
Table 1

Optical property and signal intensity of C-POSS in various concentrated methanol

Methanol (wt%)	Polarity ^a E_T (kcal/mol)	Φ_{350} ($\times 10^2$) ^b	Emission intensity (a.u.) ^c	^{19}F NMR signal height (a.u.)
10	62.2	0.809	263	n.d. ^d
25	60.3	0.609	168	n.d. ^d
50	58.3	0.499	141	n.d. ^d
75	56.8	0.378	62	25
100	55.5	0.385	62	32

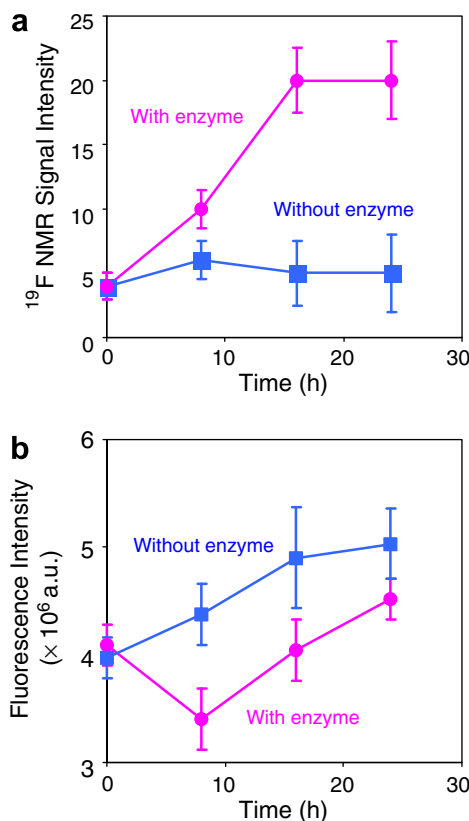
^a Ref. 11.^b Absolute fluorescence quantum yields were determined from the solution containing 25 μM C-POSS with various concentrated methanol in 50 mM sodium phosphate (pH 7.0) with the excitation at 350 nm at 25 °C.^c Emission intensity at 500 nm in Figure 1.^d n.d. = not determined.**Figure 1.** Fluorescence spectra of the sample containing 25 μM C-POSS with 10 wt% (light green line), 25 wt% (green line), 50 wt% (dark green line), 75 wt% (blue green line), and 100 wt% (blue line) methanol in 50 mM sodium phosphate buffer (pH 7.0) were measured at 25 °C with the excitation at 350 nm.**Figure 2.** Multimodal imaging of the sample containing C-POSS with various concentrated methanol. (a) The fluorescence image of the sample containing 25 μM C-POSS in 50 mM sodium phosphate buffer (pH 7.0) was obtained using a transilluminator (365 nm). (b) ^{19}F NMR spectra of the solutions containing 250 μM C-POSS with various concentrated methanol in 50 mM sodium phosphate buffer (pH 7.0).

ing 25 μM C-POSS in 50 wt% methanol, we obtained the cluster with the hydrodynamic radius $r_H = 27 \pm 4$ nm, which was significantly larger than the van der Waals radius of the C-POSS calcu-

**Figure 3.** Hydrodynamic radius of C-POSS (25 μM) with 10 (circular dots), 25 (square dots), and 50 wt% (triangular dots) methanol in 50 mM sodium phosphate buffer (pH 7.0) at 25 °C.

lated from the computer modeling (~ 1.5 nm). The larger r_H values were observed from the sample with 25 and 10 wt% methanol ($r_H = 41 \pm 7$ and 855 ± 128 nm, respectively). DLS experiments showed the cluster formation of C-POSS depended on polarity in the methanol–water solvent system.

The fluorescence decay of C-POSS or **2** in the presence of 10 wt% methanol represents that the POSS core could contribute to the

**Figure 4.** Time-course of signal changing in the enzymatic reaction. The samples (500 μL) containing 250 μM pC-POSS were incubated in the absence (square dots) and presence (circular dots) of AP (5 U) in 50 mM sodium phosphate, 25 mM Tris-HCl, and 0.05 mM EDTA (pH 7.0) at 37 °C. (a) The ^{19}F NMR signal intensity was evaluated using trifluoroacetic acid as a standard. (b) The samples were diluted to 25 μM pC-POSS for the fluorescence measurements after the enzymatic reaction, and the fluorescence intensity was monitored at 25 °C with the excitation at 350 nm.

elongation of the lifetime of the emission.¹⁵ In the variable-temperature fluorescence measurement, significant annihilation of the emission band at 500 nm was observed by heating, in which C-POSS could less aggregate because of too high temperature.¹⁶ These data including the results of DLS experiments are summarized that the cluster formation of C-POSS would be dominated by polarity, and the steric hindrance and the low tumbling mode of C-POSS could effectively prevent the free rotation of C-POSS, which results in the enhancement of the emission of CCVJ and the suppressing of the ¹⁹F NMR signals.

For the dual monitoring of the enzymatic reaction with ¹⁹F NMR and fluorescence, we prepared the phosphate ester-modified C-POSS (pC-POSS). The dispersion state of pC-POSS was altered by the enzymatic digestion of the hydrophobic phosphoramidate groups which can be cleaved by alkaline phosphatase (AP).^{17,18} After enzymatic reaction, the water-solubility of pC-POSS could be enhanced, followed by the increasing of ¹⁹F NMR signals and the decreasing of fluorescence emission of pC-POSS. The reaction mixtures containing 250 μM pC-POSS and AP in 100 mM Tris–HCl buffer (pH 8.0) were incubated at 37 °C, and ¹⁹F NMR signals and emission intensity of the reaction solution were measured (Fig. 4). The ¹⁹F NMR signal increased and saturated after 16 h incubation. In the absence of the enzyme, slight signal enhancement was observed. In contrast, fluorescence intensity of the sample containing AP correspondingly decreased after incubation. These orthogonal signal behaviors between ¹⁹F NMR signal and fluorescence corresponded to the results of the polarity changing experiments. Moreover, these results suggest that our strategy might be applicable to monitor various reactions and events.

3. Conclusion

In conclusion, we present here the ratiometric multimodal chemosensors for fluorescence and ¹⁹F NMR using the multi-functionalized POSS not only for monitoring the solvent polarity and the enzymatic reaction. Our strategy could be applied to the sensing of not only pH via hydrolysis but also other kinds of enzymes such as nucleases and proteases by the modulation with the functional groups. This manuscript proposes one example for the construction of intelligent probes for in vivo imaging.

4. Experimental

4.1. General information

¹H NMR and ¹³C NMR spectra were measured with JEOL EX-400 (400 MHz for ¹H and 100 MHz for ¹³C) spectrometer. ¹⁹F and ²⁹Si NMR spectra were measured with JEOL JNM-A400 (370 MHz for ¹⁹F and 80 MHz for ²⁹Si) spectrometer. Coupling constants (*J* value) are reported in hertz. The chemical shifts are expressed in ppm downfield from tetramethylsilane, using residual chloroform ($\delta = 7.24$ in ¹H NMR, $\delta = 77.0$ in ¹³C NMR) as an internal standard and trifluoroacetic acid in CDCl₃ as an external standard. Masses of the modified POSS were determined with a MALDI-TOF mass spectroscopy (acceleration voltage 21 kV, negative mode) with DHB (2,5-dihydroxybenzoic acid) as a matrix. The fluorescence spectra were measured by using Perkin Elmer LS50B at 25 °C. Dynamic light scattering (DLS) measurements were performed on an Otsuka FPAR-1000 apparatus at 25 °C. The dialysis membrane (2000 MWCO) was obtained from PIERCE.

4.1.1. Synthesis of octaammonium POSS (1)⁹

(3-Aminopropyl)triethoxysilane (100 mL, 0.427 mol) and 35–37% HCl (135 mL) in MeOH (800 mL) produced **1** as a white precipitate after 2 days at room temperature. The crude product obtained

after filtration, washing with cold MeOH, and drying. The product was spectroscopically pure in 30% yield (18.8 g). Recrystallization from hot MeOH afforded **1** (4.29 g, 3.66 mmol, 7%) as a white solid. ¹H NMR ((CD₃)₂SO, 25 °C): δ 8.23 (s, 24H), 2.76 (t, 16H), 1.71 (m, 16H), 0.72 (t, 16H). ¹³C NMR ((CD₃)₂SO, 25 °C): δ 40.53, 20.13, and 7.96. ²⁹SiNMR ((CD₃)₂SO, 25 °C): δ –66.4 (s).

4.1.2. Synthesis of C-POSS (3)

The molecular rotor CCVJ **3** was prepared according to the reference.⁸ To a suspension of octaammonium POSS **1** (500 mg, 0.43 mmol) and ethyl trifluoroacetate (355 μL, 2.98 mmol) in methanol (20 mL), triethylamine (2 mL, 14.4 mmol) was added, and the reaction mixture was stirred at room temperature for 3 h. The resulting mixture was evaporated, and the crude products were directly used in the next step. The compound **2** (200 mg, 0.75 mmol) and 4-(4,6-dimethoxy-1,3,5-triazin-2-yl)-4-methylmorpholinium chloride (DMT-MM) (273.5 mg, 0.86 mmol) was added to the solution in 20 mL of methanol, and the resulting mixture was stirred for 24 h at room temperature. The evaporation of volatiles produced yellow solid of crude C-POSS **3**. The crude product was purified by dialysis for removing impurities except POSS species and 164 mg (0.091 mmol, 21%) of **3** was obtained as a yellow powder. The resulting product contained a trace amount of the modified POSS which have six trifluoroacetyl groups and two CCVJ moieties or seven trifluoroacetyl groups as byproducts. ¹H NMR (CD₃OD, 25 °C): δ 7.84 (s, 1H), 7.42 (s, 2H), 3.34 (m, 16H), 3.24 (br, 4H), 2.71 (br, 4H), 1.94 (br, 4H), 1.70 (m, 16H), 0.71 (m, 16H). ¹³C NMR (CD₃OD, 25 °C): δ 159.18, 158.81, 132.79, 132.02, 131.44, 131.32, 121.79, 119.61, 118.93, 116.08, 113.22, 51.00, 42.98, 42.94, 28.54, 23.70, 23.37, 23.18, 22.15, 9.61, and 9.12. FAB-MASS: calcd for C₅₄H₇₁F₂₁N₁₀O₂₀Si₈, M⁺ *m/z* 1802.2665; found 1802.2677.

4.1.3. Synthesis of pC-POSS (4)

To a suspension of octaammonium POSS **1** (500 mg, 0.43 mmol) and ethyl trifluoroacetate (254 μL, 2.15 mmol) in methanol (20 mL), triethylamine (2 mL, 14.4 mmol) was added, and the reaction mixture was stirred at room temperature for 3 h. Subsequently, the compound **2** (154.6 mg, 0.58 mmol) DMT-MM (276.5 mg, 0.87 mmol) was added to a solution, and then the resulting mixture was stirred for 24 h at room temperature. The solution was evaporated followed by addition of chloroform (10 mL), and then methylphosphinic dichloride (114.3 mg, 0.86 mmol) was added. The resulting mixture was stirred for additional 24 h at room temperature, and then the reaction was terminated by addition of methanol (10 mL). The reaction solution was evaporated to produce red solid of crude **4**. The dialysis in water for removing impurities except POSS species gave 235.1 mg of pure **4** (0.131 mmol, 30%) as a red powder. The resulting product contained a trace amount of the modified POSS which have the different number of trifluoroacetyl group, the CCVJ moiety, and dimethoxymethylphosphate group as byproducts. ¹H NMR (CD₃OD, 25 °C): δ 7.78 (s, 1H), 7.37 (s, 2H), 3.98 (s, 6H), 3.30 (m, 20H), 2.65 (br, 4H), 1.89 (br, 4H), 1.67 (m, 16H), 1.45 (s, 6H), 0.66 (m, 16H). ¹³C NMR (CD₃OD, 25 °C): δ 174.84, 174.69, 159.54, 159.18, 158.81, 158.53, 158.45, 158.17, 153.79, 152.82, 149.37, 149.12, 132.79, 132.54, 132.50, 132.02, 121.79, 119.61, 119.18, 119.05, 118.93, 118.83, 118.79, 116.08, 115.95, 113.22, 113.04, 112.05, 56.12, 51.00, 50.99, 42.94, 42.87, 28.59, 28.47, 23.18, 23.18, 22.15, 22.01, 16.83, 9.61, 9.42. MALDI-TOF-MS [(M+H)⁺], calcd. 1796.90; found 1796.84.

4.2. Fluorescence measurements

The fluorescence emission of C-POSS solution (25 μM) in 50 mM sodium phosphate buffer (pH 7.0) with various concen-

trated methanol with the excitation at 350 nm was monitored using a Perkin Elmer LS50B equipped with a Peltier temperature controller using 1 cm path length cell. The excitation bandwidth was 1 nm. The emission bandwidth was 1 nm. For taking fluorescence imaging, the samples were illuminated with a 365 nm transilluminator.

4.3. UV absorption measurements

The solutions were prepared as described in the fluorescence measurement experiment. Absorption spectra were obtained by a Shimadzu UV-3600 spectrophotometer 25 °C using 1 cm path length cell.

4.4. DLS measurements

The DLS measurements of the samples containing 25 μ M C-POSS in various concentrated methanol and 50 mM sodium phosphate buffer (pH 7.0) were carried out at 90° scattering angle and 25 ± 0.2 °C using a FPAR-1000 particle analyzer with a He-Ne laser as a light source. The CONTIN program was used for data analysis to extract information on the average hydrodynamic size r_H .

4.5. Fluorescence lifetime study

The solutions were prepared as described in the fluorescence measurement experiment. Fluorescence decay was measured by a two-dimensional photon-counting method with the picosecond fluorescence lifetime measurement system (C4780, Hamamatsu). A N₂ laser (390 nm) was used as the excitation light source. The fluorescence emission was collected at 500 nm.

4.6. Enzymatic reactions

The reaction mixtures (500 μ L) containing 250 μ M pC-POSS and AP (5 U) in 50 mM sodium phosphate, 25 mM Tris-HCl, 10 vol% methanol, and 0.05 mM EDTA (pH 7.0) were incubated at 37 °C. The reaction was terminated by adding 50 μ L of 10 mM EDTA to the reaction mixture, and then ¹⁹F NMR spectra were taken with JEOL JNM-A400 (370 MHz). The fluorescence intensity of the diluted samples (25 μ M pC-POSS) was measured under excitation at 350 nm.

Acknowledgments

This study was conducted as a part of the project, 'R&D of Molecular Imaging Equipment for Malignant Tumor Therapy Support,' supported by NEDO (New Energy and Industrial Technology Development Organization). We thank Prof. Y. Tsuji and Dr. T. Fujiwara for the measurement of ¹⁹F NMR. We thank Prof. I. Hamachi and Mr. S. Fujishima for taking the fluorescence image.

Supplementary data

Supplementary data associated with this article can be found, in the online version, at doi:10.1016/j.bmc.2008.10.016.

References and notes

- (a) Zimmermann, U.; Nöth, U.; Gröhn, P.; Jork, A.; Ulrichs, K.; Lutz, J.; Haase, A. *Artif. Cells Blood Substit. Immobil. Biotechnol.* **2000**, 28, 129; (b) Yu, J.; Kodibagkar, V. D.; Cui, W.; Mason, R. P. *Curr. Med. Chem.* **2005**, 12, 819; (c) Higuchi, M.; Iwata, N.; Matsuba, Y.; Sato, K.; Sasamoto, K.; Saido, T. C. *Nat. Neurosci.* **2005**, 8, 527; (d) Ahrens, E. T.; Flores, R.; Xu, H. Y.; Morel, P. A. *Nat. Biotechnol.* **2005**, 23, 983; (e) Maki, J.; Masuda, C.; Morikawa, S.; Morita, M.; Inubushi, T.; Matsusue, Y.; Taguchi, H.; Tooyama, I. *Biomaterials* **2007**, 28, 434; (f) Morawski, A. M.; Winter, P. M.; Yu, X.; Fuhrhop, R. W.; Scott, M. J.; Hockett, F.; Robertson, J. D.; Gaffney, P. J.; Lanza, G. M.; Wickline, S. A. *Magn. Reson. Med.* **2004**, 52, 1255; (g) Mizukami, S.; Takikawa, R.; Sugihara, F.; Hori, Y.; Tochio, H.; Waelchli, M.; Shirakawa, M.; Kikuchi, K. *J. Am. Chem. Soc.* **2008**, 130, 794; (h) Oishi, M.; Sumitani, S.; Nagasaki, Y. *Bioconjugate Chem.* **2007**, 18, 1379; (i) Cui, W.; Otten, P.; Li, Y.; Koenenman, K. S.; Yu, J.; Mason, R. P. *Magn. Reson. Med.* **2004**, 51, 616.
- (a) Zhang, X.; Lovejoy, K. S.; Jasanoff, A.; Lippard, S. J. *Proc. Natl. Acad. Sci. U.S.A.* **2007**, 104, 10780; (b) Weissleder, R.; Pittet, M. J. *Nature* **2008**, 452, 580; (c) Alric, C.; Taleb, J.; Le Duc, G.; Mandon, C.; Billotey, C.; Le Meur-Herland, A.; Brochard, T.; Vocanson, F.; Janier, M.; Perriat, P.; Roux, S.; Tillement, O. *J. Am. Chem. Soc.* **2008**, 130, 5908; (d) Li, C.; Winnard, P. T., Jr.; Takagi, T.; Artemov, D.; Bhujwalla, Z. M. *J. Am. Chem. Soc.* **2006**, 128, 15072; (e) Cicchetti, F.; Gross, R. E.; Bulte, J. W. M.; Owen, M.; Chen, I.; Saint-Pierre, M.; Wang, X.; Yu, M.; Brownell, A.-L. *Contrast Media Mol. Imaging* **2007**, 2, 130; (f) Bridot, J.-L.; Faure, A.-C.; Laurent, S.; Riviere, C.; Billotey, C.; Hiba, B.; Janier, M.; Josserand, V.; Coll, J.-L.; Vander Elst, L.; Muller, R.; Roux, S.; Perriat, P.; Tillement, O. *J. Am. Chem. Soc.* **2007**, 129, 5076; (g) Hattori, Y.; Asano, T.; Niki, Y.; Kondoh, H.; Kirihata, N.; Yamaguchi, Y.; Wakamiya, T. *Bioorg. Med. Chem.* **2006**, 14, 3258.
- (a) Janjic, J. M.; Srinivas, M.; Kadayakkara, D. K. K.; Ahrens, E. T. *J. Am. Chem. Soc.* **2008**, 130, 2832; (b) Xia, M.; Kodibagkar, V. D.; Liu, H.; Mason, R. P. *Phys. Med. Biol.* **2006**, 51, 45.
- Jacob, F. In *Molecular Fluorescence, Principles and Applications*; Valeur, B., Ed.; Wiley-VCH: Weinheim, 2002; p 282.
- (a) Nolan, E. M.; Lippard, S. J. *J. Am. Chem. Soc.* **2007**, 129, 5910; (b) Zhang, Y.; Guo, X.; Si, W.; Jia, L.; Qian, X. *Org. Lett.* **2008**, 10, 473; (c) Nakata, E.; Koshi, Y.; Koga, E.; Katayama, Y.; Hamachi, I. *J. Am. Chem. Soc.* **2005**, 127, 13253; (d) Ojida, A.; Nonaka, H.; Miyahara, Y.; Tamaru, S.; Sada, K.; Hamachi, I. *Angew. Chem. Int. Ed.* **2006**, 45, 5518; (e) Komatsu, K.; Urano, Y.; Kojima, H.; Nagano, T. *J. Am. Chem. Soc.* **2007**, 129, 13447; (f) Kikuchi, K. *Bioimages* **2004**, 12, 55; (g) Kikuchi, K.; Takakusa, H.; Nagano, T. *Trends Anal. Chem.* **2004**, 23, 407; (h) Demchenko, A. P. *Lab Chip* **2005**, 5, 1210; (i) Park, E. J.; Reid, K. R.; Tang, W.; Kennedy, R. T.; Kopelman, R. J. *Mater. Chem.* **2005**, 15, 2913; (j) Badugu, R.; Lakowicz, J. R.; Geddes, C. D. *J. Am. Chem. Soc.* **2005**, 127, 3635; (k) Peng, X.; Du, J.; Fan, J.; Wang, J.; Wu, Y.; Zhao, J.; Sun, S.; Xu, T. *J. Am. Chem. Soc.* **2007**, 129, 1500; (l) Kermis, H. R.; Kostov, Y.; Harms, P.; Rao, G. *Biotechnol. Prog.* **2002**, 18, 1047.
- (a) Laine, R. M.; Choi, J.; Lee, I. *Adv. Mater.* **2001**, 13, 800; (b) Wang, X.; Naka, K.; Itoh, H.; Chujo, Y. *Chem. Lett.* **2004**, 33, 216.
- Tanaka, K.; Kitamura, N.; Naka, K.; Chujo, Y. *Chem Commun.* **2008**. doi:10.1039/b815022b.
- Haidekker, M. A.; Ling, T.; Anglo, M.; Stevens, H. Y.; Frangos, J. A.; Theodorakis, E. A. *Chem. Biol.* **2001**, 8, 123.
- (a) Gravel, M.-C.; Laine, R. M. *Am. Chem. Soc. Polym. Prepr.* **1997**, 38, 155; (b) Feher, F. J.; Wyndham, K. D. *Chem. Commun.* **1998**, 323; (c) Gravel, M.-C.; Zhang, C.; Dinderman, M.; Laine, R. M. *Appl. Organomet. Chem.* **1999**, 13, 329.
- Synthetic details are shown in Section 4.
- Dimroth, K.; Reichardt, C. Z. *Anal. Chem.* **1966**, 215, 344.
- Chauhan, S.; Syal, V. K.; Chauhan, M. S.; Sharma, P. J. *Mol. Liq.* **2007**, 136, 161.
- See Figure S1 in the Supporting Information.
- See Figure S2 in the Supporting Information.
- See Table S1 in the Supporting Information.
- See Figure S3 in the Supporting Information.
- Schematic illustration for the detection mechanism of pC-POSS is shown in Figure S4 in the Supporting Information.
- Simoncsits, A.; Tomasz, J. *Nucleic Acids Res.* **1975**, 2, 1223.